

Thermal conductivity of B-DNA

Vignesh Mahalingam^{a,1} and Dineshkumar Harursampath^{a,2}

^aDepartment of Aerospace Engineering, Indian Institute of Science, Bangalore, 560012, India

This manuscript was compiled on October 1, 2020

The thermal conductivity of B-form double-stranded DNA (dsDNA) of the Drew-Dickerson sequence d(CGCGAATTCGCG) is computed using classical Molecular Dynamics (MD) simulations. In contrast to previous studies, which focus on a simplified 1D model or a coarse-grained model of DNA to improve simulation times, full atomistic simulations are employed to understand the thermal conduction in B-DNA. Thermal conductivity at different temperatures from 100 to 400 K are investigated using the Einstein Green-Kubo equilibrium and Müller-Plathe non-equilibrium formalisms. The thermal conductivity of B-DNA at room temperature is found to be 1.5 W/m·K in equilibrium and 1.225 W/m·K in non-equilibrium approach. In addition, the denaturation regime of B-DNA is obtained from the variation of thermal conductivity with temperature. It is in agreement with previous works using Peyrard-Bishop Dauxois (PBD) model at a temperature of around 350 K. The quantum heat capacity (C_{vq}) has given the additional clues regarding the Debye and denaturation temperature of 12-bp B-DNA.

B-DNA | thermal conductivity | heat capacity | molecular dynamics | Green-Kubo | Müller-Plathe

Probing thermal conduction in shorter length scales using computations gives us a fundamental understanding of the link between structure and phenomena. DNA satisfies the low thermal conductivity requirements for building molecular thermoelectric devices (1). This was a motivation for this study. In an experiment to find the thermal conduction of DNA-gold composite where λ -DNA coated with gold nanoparticles (2), the thermal conductivity (κ) was found to be 150 W/m·K. The later works have cited that gold primarily contribute to this high value of thermal conductivity and have mentioned that the ultra-low thermal conductivity of DNA (3–5). An experiment using a new transient electrothermal technique with crystalline DNA composite fibers in NaCl solution, has suggested that this might indeed be the case as the thermal conductivity found for the fibers are low around 0.25–0.85 W/m·K (3, 4).

The earlier computational works use the Peyrard-Bishop-Dauxois (PBD) model which is a simplified 1-D non-linear bead spring model (6). This model has been used to understand DNA dynamics and to find the denaturation point of DNA (7). The denaturation regime of DNA was found to be around 350 K and thermal conductivity of the DNA in (8) at 300 K is 1.8 mW/m·K. This value is much lower than that of poly(G) DNA (≈ 0.3 W/m·K) obtained using a 12-coarse grained (12-CG) model (5). The disagreement raises the question of the validity of thermal conductivity computed using PBD model. A few infinite chains formed by permuting Adenine (A) and Guanine (G) sequences-poly(A), poly(G), poly(AG), poly(A₂G₂), poly(A₂₀₀G₂₀₀) are investigated using PBD model and it was found that the denaturation point can be shifted depending on the sequence (9). Additionally, the thermal conductance ratio $R = \kappa_H/\kappa_L$, which is defined as the high thermal conductivity to low thermal conductivity

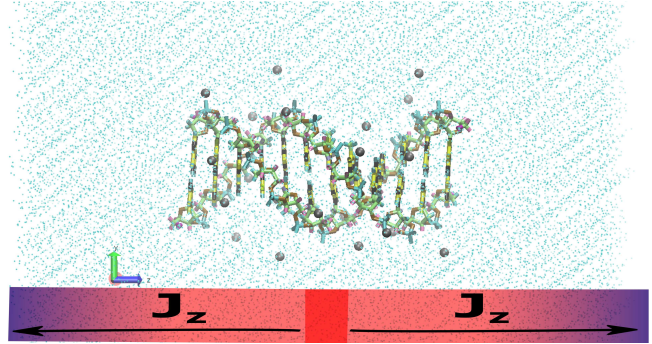


Fig. 1. The simulated B-DNA structure is in a water box with Na^+ ions. The B-DNA has a total length of 40.8 Å and a radius of 10 Å and is colored according to different atom types. Also shown is the non-equilibrium Müller-Plathe scheme where the red region with higher temperature swaps kinetic energies with blue regions with lower temperatures.

of various sequences is quantified to analyze thermal switching in DNA. The sequence poly(A₂G₂) seemed to have higher the thermal conductance ratio than poly(A) and poly(G) sequences. Again, the thermal conductance values were extremely lower, probably owing to the PBD model (9). The PBD model has also been used to understand the improving heat conduction through external force (10). As an extension of this, DNA switching was studied by considering one end of DNA helical turn as drain, another end as source and the central region as gate(11). An all-atom picture resolves the discrepancies in understanding the fundamental nature of thermal conduction in a DNA. Hence, the water and Na^+ ions are considered as the stabilizing media and only the thermal conductivity of B-DNA is calculated.

Significance Statement

The thermal conductivity of B-form double-stranded DNA (dsDNA) of the Drew-Dickerson sequence d(CGCGAATTCGCG) is computed using classical Molecular Dynamics (MD) simulations. In contrast to previous studies, which focus on a simplified 1D model or a coarse-grained model of DNA to improve simulation times, full atomistic simulations are employed to understand the thermal conduction in B-DNA. Thermal conductivity at different temperatures from 100 to 400 K are investigated using the Einstein Green-Kubo equilibrium and Müller-Plathe non-equilibrium formalisms.

Vignesh Mahalingam performed research and Vignesh Mahalingam, Dineshkumar Harursampath wrote the paper together

The authors declare no conflict of interest.

²To whom correspondence should be addressed. E-mail: vigneshmiisc.ac.in

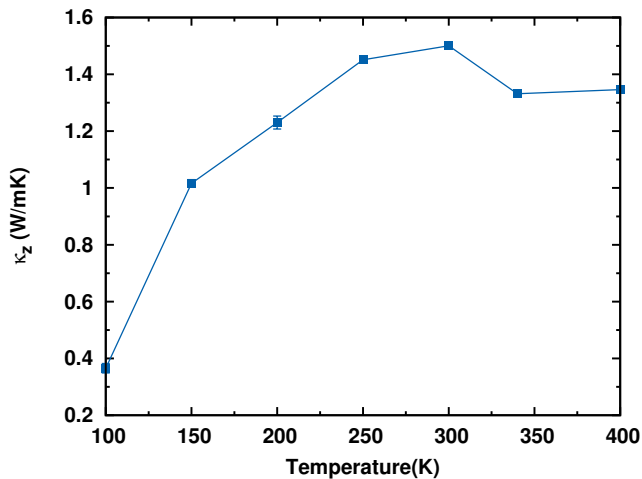


Fig. 2. Thermal conductivity of B-DNA along the length of DNA as a function of temperature (4).

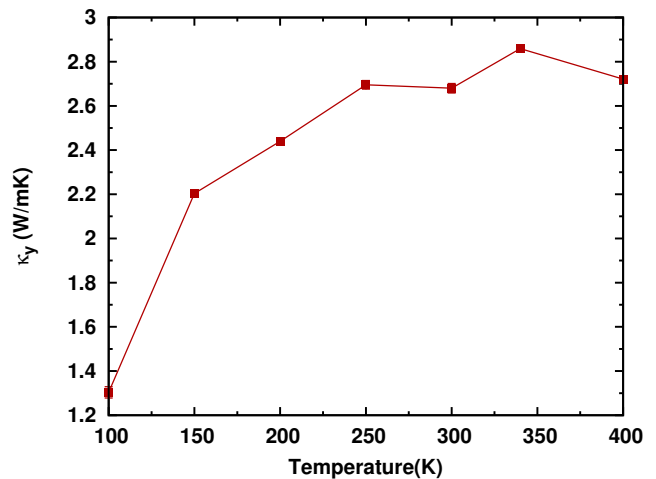


Fig. 3. Thermal conductivity of B-DNA along base-pairs κ_y as a function of temperature.

Results and discussion

Thermal conductivity using Green-Kubo equilibrium method.

The thermal conductivity of B-DNA is calculated using the equilibrium GK method as in equation (2). This requires the calculation of heat-heat auto-correlation function (HCAF) from heat current using equation (3) and this settles to an equilibrium value. The thermal conductivity value obtained at 300 K along the length of DNA after it has settled to an equilibrium value for 10 ns. All equilibrium GK thermal conductivity values at different temperature are obtained similarly. The thermal conductivity of the dsDNA sequence along its length as a function of temperature is shown in Figure 2. The thermal conductivity increases as a function of temperature and eventually saturates around 350 K.

The equilibrium method also allows us to calculate the heat flux along the other directions such as those between the strands as shown in Figure 3. These thermal conductivities are inaccessible to experiments at such shorter strand lengths. Interestingly, the heat transfer along base pairs between backbone is higher than that along the strand. No parallels exist in reported literature about the heat conduction between strands, although (5) has mentioned that the heat conduction along the length is primarily due to sugar-phosphate backbone. The classical treatment here has not accounted for the transfer of heat between base pairs by tunneling. Nevertheless, it is evident from Figure 3 that more heat can be transferred along base pairs than along the length of phosphate backbone.

Power density spectrum. To understand the molecular origin of the temperature dependence of the thermal conductivity of the DNA, the Density of States (DoS) of the 12-bp B-DNA have been calculated using a 2-point (2pt) code (12–14) and have been plotted in Figure 4. Only continuous low frequency modes can be seen till 800 cm^{-1} (Debye frequency, ω_D). In an earlier work on poly-G DNA (5), the DoS spectrum had a gap with no modes between 200 cm^{-1} and 300 cm^{-1} . Moreover, few modes existed beyond this gap till 400 cm^{-1} . No such gap is seen in the spectrum between optical and acoustic modes. No high frequency modes has been observed in both

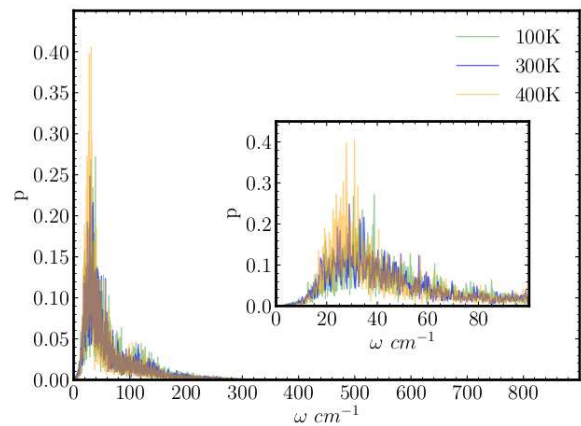


Fig. 4. Power spectrum density of B-DNA at 300 K, 100 K and 400 K.

this work and in earlier work (5), meaning that the phonon modes have large wavelengths and hence are scattered at the dsDNA boundaries. Around the denaturation temperature, the DNA strands separate, and the thermal conductivity saturates. It is possible to compute the Debye temperature, T_D from this spectrum by using $T_D = \hbar\omega_D/k_B$, where \hbar and k_B are reduced Planck's constant and Boltzmann constant, respectively. Substituting ω_D to be 723 cm^{-1} as it the last available frequency mode, $T_D \approx 165\text{ K}$.

Using the DoS shown in Figure 4, also computed is the quantum molar specific heat capacity (C_{vq}) of the dsDNA (Figure 5). The resulting heat capacity is plotted as a function of temperature. The peaks in heat capacity at 200 K and 273 K in Figure 5 are probably due to water as similar features can be seen in water heat capacity at the same temperatures in Figure 6. The peak at 150 K is close to the calculated Debye temperature (165 K) of DNA. The peak around 350 K ought to correspond with the denaturation regime, where the transition from double strand to two single strands happens (15). It is till this point that the thermal conductivity increases and beyond which thermal conductivity saturates.

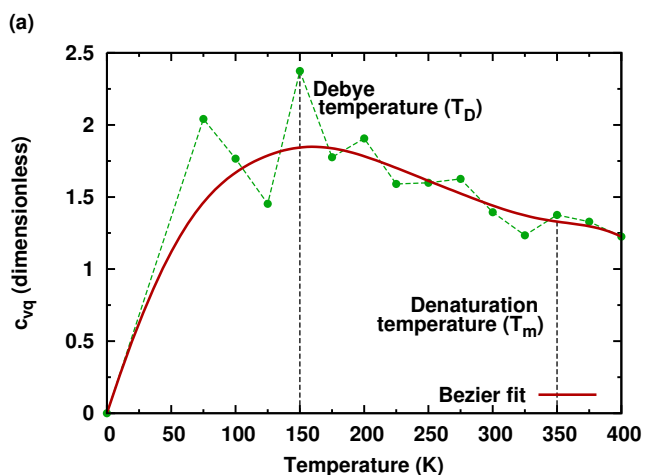


Fig. 5. Quantum heat capacity (C_{vq}) of B-DNA as a function of temperature.

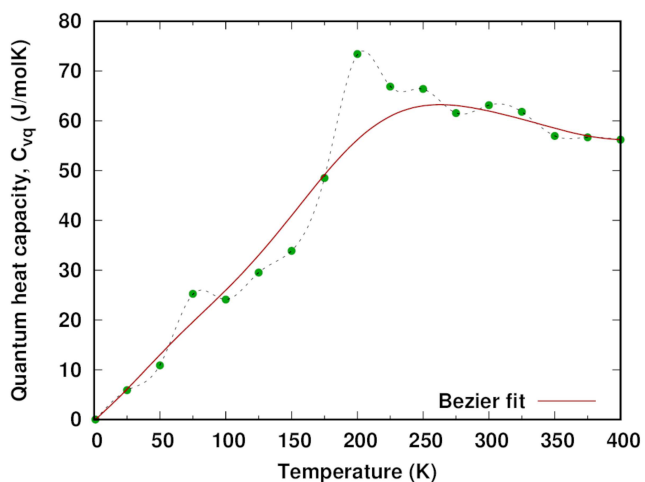


Fig. 6. Quantum heat capacity (C_{vq}) of TIP3P water as a function of temperature.

A similar study (8) has described the same phenomenon and it is mentioned that the increase in thermal conductivity is strongly correlated with the anharmonicity in the bond between the complementary base pairs till there is effectively no contact between the complementary base pairs.

Thermal conductivity using Reverse Non-Equilibrium Molecular Dynamics (RNEMD) method. A non-equilibrium MD approach (16) is also used to understand the low thermal conductivity obtained earlier using equilibrium formulation. Here, a temperature gradient can be set along the length of B-DNA and surrounding water box. The temperature profile across the surrounding water clearly has a gradient between the center hot region and cold regions on either side. Figures 7 and 8 shows the water and DNA temperature profiles, respectively.

The thermal conductivity κ due to a linear temperature gradient between the DNA ends (between 22.5 and 67.5 Å) is given as

$$\kappa_z = \frac{\left(\frac{Q}{At}\right)}{(\partial T/\partial z)}, \quad [1]$$

where Q is the heat exchange between hot and cold regions, A is the cross-sectional area of the water box and t is the time for

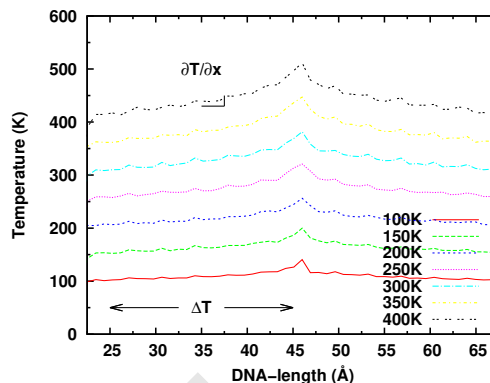


Fig. 7. Temperature profile across the water box which has B-DNA along z-direction

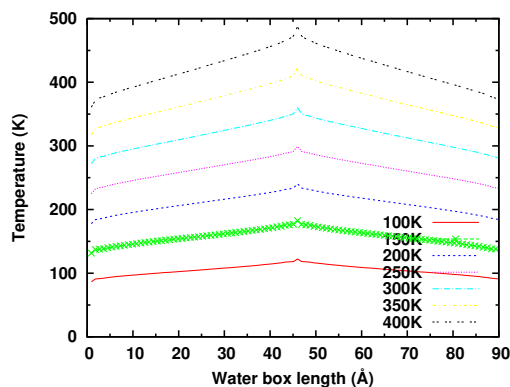


Fig. 8. Temperature profile across the 12-bp B-DNA in RNEMD simulation along z-direction

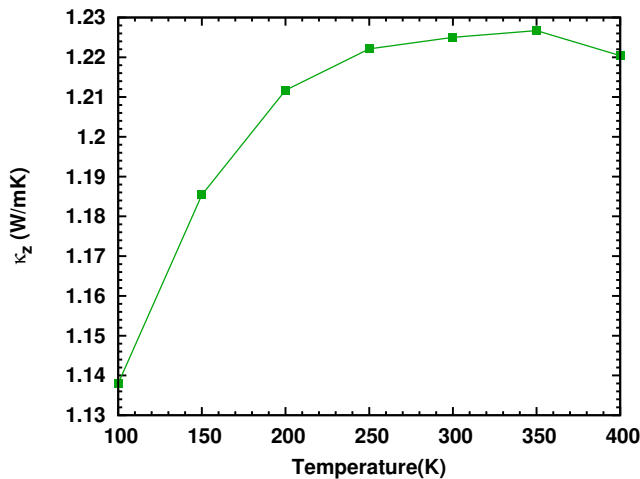


Fig. 9. Thermal conductivity versus temperature for 12-bp B-DNA in RNEMD simulation. Inset shows the Green-Kubo values plotted in Figure 2.

heat exchange. The temperature gradient is computed across B-DNA from the temperature profile in Figure 8. Caution was exercised in calculating the temperature profile as constrained SHAKE atoms were excluded and a mild Berendsen thermostat was used (17). Figure 9 shows the temperature dependence of the thermal conductivity using this method and the profile similar to GK thermal conductivity (Figure 2).

Till denaturation there is an increase in thermal conductivity κ and heat capacity (C) of B-DNA with respect to temperature. This is attributed to increase of phonon density with respect to temperature (4) as $\kappa = \frac{Cv^2\tau_r}{3}$ in the single time relaxation approximation. Moreover, it can be seen from Figure 4 that only low frequency (long wavelength) soft modes are available in DNA allowing this classical approximation to be valid. The heat capacity (C) of B-DNA also increases as Debye law states: $C_{vq} \propto T^3$ (Refer Figure 5). It is being assumed that the phonon velocity (v) remains almost constant with temperature and the relaxation time $\tau_r \propto T^{-1}$ (4). Hence, the thermal conductivity initially increases almost quadratically with respect to temperature till the DNA strands separate. The thermal conductivity of the DNA-gold composite is found to be 150 W/m-K (2), whereas recent estimates of the thermal conductivity of DNA-water composite mixture via equilibrium and non-equilibrium MD were 0.381 W/m-K and 0.373 W/m-K, respectively (18). Our results suggest that there is a definite contribution of gold and water to the thermal conductivity of the composite mixture in these works and the thermal conductivity of DNA is somewhere close to the reported values in this work.

1. Discussion

We have examined the thermal conductivity of 12-bp B-DNA, the most common form of DNA from GK calculation from RNEMD calculation. Both calculations show an increase in thermal conductivity till denaturation temperature. The full atom description as opposed to coarse grained or 1D non-linear chain models indicate the regions where the models succeed and fail. The thermal conductivity obtained using PBD models needs to be refined as they seem to be very low. Nevertheless, all models predict the denaturation regime close

to 350 K, where the thermal conductivity saturates with increase in temperature. The 2pt-calculations show that the Debye temperature is consistent with the earlier works (5, 8, 9). The engineering of thermal conductivity, based on the base-pair sequences along the long lengths, might play a role in its usage as a molecular thermoelectric device operating at room temperature. This work lays the foundation for an all-atom study of DNA thermal conductivity. Building further using the methods here would give us insight into the dependence of thermal conductivity on base-pair sequences from all-atom perspective. The thermal conductivity computed here might be a necessary validity check for coarse-grained DNA models.

Materials and Methods

All the calculations are performed on the 12-base pair (bp) B-DNA of Drew-Dickerson sequence d(CGCGAATTCGCG) (19). Nucleic Acid Builder (NAB) module of AMBERTOOLS18 (20) is used to build the initial structures of the double stranded (ds) DNA. The dsDNA is then placed in a bath of TIP3P water box (21) using xleap module of AMBERTOOLS18 software package. A water box with dimensions of $65 \text{ \AA} \times 65 \text{ \AA} \times 90 \text{ \AA}$ ($x \times y \times z$) is chosen to ensure 15 \AA solvation shell around the B-DNA. 22 Na^+ ions are added at the lowest electrostatic potential locations to the solvated dsDNA system. DNA OL15 force-field (22) is used. This has parmbsc0 (23) and OL15 (22) corrections to the ff99 force-field (24) to consider the bonded and non-bonded interactions of the dsDNA. Joung-Cheatham parameter (25) set is used to consider the interaction of monovalent Na^+ ions with TIP3P water and dsDNA. After preparing the initial system using AMBERTOOLS18 (20), LAMMPS (26) software module is used for all further simulations. The whole solvated dsDNA system is energy minimized using first 5000 steps of steepest descent and 5000 steps of conjugate gradient keeping the B-DNA restrained with a force of 500 kcal/mol \AA . The DNA is then slowly released into water by reducing the restraint from 20 kcal/mol \AA to 0 kcal/mol \AA in 5 cycles of the steepest descent and conjugate gradient minimization steps. All the atoms are then assigned velocities according to Maxwell-Boltzmann distribution. Throughout the MD simulation, the DNA has a small restraint of 1 kcal/mol \AA to prevent the same from changing its orientation whilst measuring thermal conductivity. SHAKE constraints (27) are applied to the hydrogen atoms, bond and angles of DNA and water with a tolerance of 10^{-4} (24). The system is equilibrated for 10 ns with Nosé-Hoover thermostat and barostats with coupling constants 0.1 ps and 1.0 ps, respectively (28–31). Finally, a production run of 20 ns for the calculation of thermal conductivity ensures that the thermal conductivity values converge. The thermal conductivity is computed using the equilibrium Green-Kubo (GK) method, where the heat-heat auto-correlation function is used to compute the thermal conductivity as (32–34):

$$\kappa_{x,y,z} = \frac{V}{k_B T^2} \int_0^\infty \langle J_{x,y,z}(0) \cdot J_{x,y,z}(t) \rangle dt, \quad [2]$$

where thermal conductivity $\kappa_{x,y,z}$ at a temperature T in a direction x , y or z is obtained from heat current $J_{x,y,z}$ in that direction. k_B is the Boltzmann constant. The heat current is obtained as

$$\mathbf{J} = \frac{1}{V} \left[\sum_i e_i v_i - \sum_i \sigma_i v_i \right] \quad [3]$$

where e_i is the total energy of an atom, v_i is the velocity of an atom, σ_i is the virial stress per atom and V is the volume of the total group of atoms. The exact volume (V) of B-DNA is computed from the atomic volumes of adenine (136.1 \AA^3), guanine (143.8 \AA^3), cytosine (113.2 \AA^3) and thymine (132.6 \AA^3) base-pair groups and sugar-phosphate (174.8 \AA^3) groups (35, 36). Each strand (left or right of B-DNA symmetrical axis) contains 4 cytosine, 4 guanine, 2 adenine and 2 thymine and 12 sugar-phosphate groups giving us the total volume of the 12-bp B-DNA to be 7326 \AA^3 . The power spectrum density or Density of States (DoS) of the 12-bp B-DNA

is obtained from a fast Fourier transform of velocity-velocity auto-correlation, $C(t)$ as

$$DoS(\nu) = \lim_{t \rightarrow \infty} \frac{1}{2k_B T} \int_{-\tau}^{\tau} C(t) e^{-2\pi\nu t} dt, \quad [4]$$

where t is correlation time window of 200 ps and ν is the frequency. Only the solid component of DoS is considered as liquid and gaseous states are not relevant for B-DNA. The canonical partition function (Q) can be constructed from DoS, with a harmonic oscillator assumption:

$$\ln Q = \int_0^{\infty} DoS(\nu) q_{HO}(\nu) d\nu, \quad [5]$$

where $q_{HO} = \frac{e^{-\beta h\nu}}{1 - e^{-\beta h\nu}}$ is the harmonic oscillator partition function, $\beta = \frac{1}{k_B T}$ and h is the Planck's constant. The entropy S^0 and the heat capacity C_{vq} are then found using the partition function and DoS as

$$S^0 = k \ln Q + \beta^{-1} \left(\frac{\partial \ln Q}{\partial T} \right)_{N,V} = k \int_0^{\infty} DoS(\nu) W^s(\nu) d\nu \quad [6]$$

$$\begin{aligned} C_{vq} &= \left(\frac{\partial S^0}{\partial T} \right) = k \left(\frac{\partial \ln Q}{\partial T} \right)_{N,V} + \beta^{-1} \left(\frac{\partial^2 \ln Q}{\partial T^2} \right)_{N,V} \\ &= k^2 \beta^{-2} \int_0^{\infty} DoS(\nu) W^C(\nu) d\nu \end{aligned} \quad [7]$$

with weighting functions

$$W^s(\nu) = \frac{\beta h\nu}{e^{\beta h\nu} - 1} \ln [1 - (e^{-\beta h\nu})], \quad [8]$$

$$W^C(\nu) = \frac{e^{-\beta h\nu}}{[1 - (e^{-\beta h\nu})]^2}. \quad [9]$$

ACKNOWLEDGMENTS. The authors thank Dr. Navaneetha Krishnan, Dr. Prabal Maiti and Abhishek Aggarwal for their fruitful discussions and suggestions.

- LL Nian, W Liu, L Bai, XF Wang, Spin caloritronics in a chiral double-strand-dna-based hybrid junction. *Phys. Rev. B* **99**, 195430 (2019).
- T Kodama, A Jain, KE Goodson, Heat conduction through a dna-gold composite. *NANO LETTERS* **9**, 2005–2009 (2009).
- Z Xu, S Xu, X Tang, X Wang, Energy transport in crystalline dna composites. *AIP ADVANCES* **4** (2014).
- Z Xu, X Wang, H Xie, Promoted electron transport and sustained phonon transport by dna down to 10 k. *Polymer* **55**, 6373 – 6380 (2014).
- AV Savin, MA Mazo, IP Kikot, LI Manevitch, AV Onufriev, Heat conductivity of the dna double helix. *Phys. Rev. B* **83**, 245406 (2011).
- M Peyrard, Nonlinear dynamics and statistical physics of DNA. *Nonlinearity* **17**, R1–R40 (2004).
- M Peyrard, AR Bishop, Statistical mechanics of a nonlinear model for dna denaturation. *Phys. Rev. Lett.* **62**, 2755–2758 (1989).
- KA Velizhanin, CC Chien, Y Dubi, M Zwolak, Driving denaturation: Nanoscale thermal transport as a probe of dna melting. *Phys. Rev. E* **83**, 050906 (2011).
- CC Chien, KA Velizhanin, Y Dubi, M Zwolak, Tunable thermal switching via DNA-based nano-devices. *Nanotechnology* **24**, 095704 (2013).
- S Behnia, R Panahinia, Ballistic induced pumping of hypersonic heat current in DNA nano wire. *EUROPEAN PHYSICAL JOURNAL B* **89** (2016).
- S Behnia, R Panahinia, Molecular thermal transistor: Dimension analysis and mechanism. *CHEMICAL PHYSICS* **505**, 40–46 (2018).
- ST Lin, M Blanco, WA Goddard, The two-phase model for calculating thermodynamic properties of liquids from molecular dynamics: Validation for the phase diagram of lennard-jones fluids. *The J. Chem. Phys.* **119**, 11792–11805 (2003).
- ST Lin, PK Maiti, WA Goddard, Two-phase thermodynamic model for efficient and accurate absolute entropy of water from molecular dynamics simulations. *The J. Phys. Chem. B* **114**, 8191–8198 (2010).
- TA Pascal, ST Lin, WA Goddard III, Thermodynamics of liquids: standard molar entropies and heat capacities of common solvents from 2pt molecular dynamics. *Phys. Chem. Chem. Phys.* **13**, 169–181 (2011).
- A Wildes, et al., Structural correlations and melting of b-dna fibers. *Phys. Rev. E* **83**, 061923 (2011).
- F Müller-Plathe, A simple nonequilibrium molecular dynamics method for calculating the thermal conductivity. *The J. Chem. Phys.* **106**, 6082–6085 (1997).
- M Zhang, E Lussetti, LES de Souza, F Müller-Plathe, Thermal conductivities of molecular liquids by reverse nonequilibrium molecular dynamics. *The J. Phys. Chem. B* **109**, 15060–15067 (2005).
- NA Jolfaei, et al., Investigation of thermal properties of dna structure with precise atomic arrangement via equilibrium and non-equilibrium molecular dynamics approaches. *Comput. Methods Programs Biomed.* **185**, 105169 (2020).
- R Dickerson, et al., The anatomy of a-, b-, and z-dna. *Science* **216**, 475–485 (1982).
- D Case, et al., Amber 2018 (2018).
- WL Jorgensen, J Chandrasekhar, JD Madura, RW Impey, ML Klein, Comparison of simple potential functions for simulating liquid water. *The J. Chem. Phys.* **79**, 926–935 (1983).
- M Zgarbova, et al., Refinement of the Sugar-Phosphate Backbone Torsion Beta for AMBER Force Fields Improves the Description of Z- and B-DNA. *JOURNAL OF CHEMICAL THEORY AND COMPUTATION* **11**, 5723–5736 (2015).
- A Pérez, et al., Refinement of the amber force field for nucleic acids: Improving the description of α/γ conformers. *Biophys. J.* **92**, 3817 – 3829 (2007).
- J Wang, P Cieplak, P Kollman, How well does a restrained electrostatic potential (RESP) model perform in calculating conformational energies of organic and biological molecules? *JOURNAL OF COMPUTATIONAL CHEMISTRY* **21**, 1049–1074 (2000).
- IS Joung, TE Cheatham, Determination of alkali and halide monovalent ion parameters for use in explicitly solvated biomolecular simulations. *The J. Phys. Chem. B* **112**, 9020–9041 (2008).
- S Plimpton, Fast parallel algorithms for short-range molecular dynamics. *J. Comput. Phys.* **117**, 1 – 19 (1995).
- JP Ryckaert, G Ciccotti, HJ Berendsen, Numerical integration of the cartesian equations of motion of a system with constraints: molecular dynamics of n-alkanes. *J. Comput. Phys.* **23**, 327 – 341 (1977).
- W Shinoda, M Shiga, M Mikami, Rapid estimation of elastic constants by molecular dynamics simulation under constant stress. *Phys. Rev. B* **69**, 134103 (2004).
- GJ Martyna, DJ Tobias, ML Klein, Constant pressure molecular dynamics algorithms. *The J. chemical physics* **101**, 4177–4189 (1994).
- M Parrinello, A Rahman, Polymorphic transitions in single crystals: A new molecular dynamics method. *J. Appl. physics* **52**, 7182–7190 (1981).
- ME Tuckerman, J Alejandre, R López-Rendón, AL Jochim, GJ Martyna, A liouville-operator derived measure-preserving integrator for molecular dynamics simulations in the isothermal-isobaric ensemble. *J. Phys. A: Math. Gen.* **39**, 5629 (2006).
- M GREEN, MARKOFF RANDOM PROCESSES AND THE STATISTICAL MECHANICS OF TIME-DEPENDENT PHENOMENA. *JOURNAL OF CHEMICAL PHYSICS* **20**, 1281–1295 (1952).
- M GREEN, MARKOFF RANDOM PROCESSES AND THE STATISTICAL MECHANICS OF TIME-DEPENDENT PHENOMENA .2. IRREVERSIBLE PROCESSES IN FLUIDS. *JOURNAL OF CHEMICAL PHYSICS* **22**, 398–413 (1954).
- R Kubo, Statistical-mechanical theory of irreversible processes. i. general theory and simple applications to magnetic and conduction problems. *J. Phys. Soc. Jpn.* **12**, 570–586 (1957).
- K Nadassy, I Tomás-Oliveira, I Alberts, J Jarin, S Wodak, Standard atomic volumes in double-stranded dna and packing in protein-dna interfaces. *Nucleic Acids Res.* **29**, 3362–3376 (2001).
- N Voss, M Gerstein, Calculation of standard atomic volumes for rna and comparison with proteins: Rna is packed more tightly. *J. Mol. Biol.* **346**, 477 – 492 (2005).